

A Novel Energy-Efficient Cross-Layer Design for Scheduling and Routing in 6TiSCH Networks

Ahlam Hannachi, Wael Jaafar, Salim Bitam, and Nabil Ouazene

Abstract—The 6TiSCH protocol stack was proposed to ensure high-performance communications in the Industrial Internet of Things (IIoT). However, the lack of sufficient time slots for nodes outside the 6TiSCH’s Destination Oriented Directed Acyclic Graph (DODAG) to transmit their Destination Advertisement Object (DAO) messages and cell reservation requests significantly hinders their integration into the DODAG. This oversight not only prolongs the device’s join time but also increases energy consumption during the network formation phase. Moreover, challenges emerge due to the substantial number of control packets employed by both the 6TiSCH Scheduling Function (SF) and routing protocol (RPL), thus draining more energy resources, increasing medium contention, and decreasing spatial reuse. Furthermore, an SF that overlooks previously allocated slots when assigning new ones to the same node may increase jitter, and more complications ensue when it neglects the state of the TSCH queue, thus leading to packet dropping due to queue saturation. Additional complexity arises when the RPL disregards the new parent’s schedule saturation during parent switching, which results in inefficient energy and time usage. To address these issues, we introduce in this paper novel mechanisms, strategically situated at the intersection of SF and RPL that are designed to balance the control packet distribution and adaptively manage parent switching. Our proposal, implemented within the 6TiSCH simulator, demonstrates significant improvements across vital performance metrics, such as node’s joining time, jitter, latency, energy consumption, and amount of traffic, in comparison to the conventional 6TiSCH benchmark.

Index Terms—Industrial IoT, TSCH, 6TiSCH, SF, RPL network formation, scheduling, routing.

I. INTRODUCTION

Amid current digital advancements, the presence of the Internet permeates nearly every aspect of our lives, spanning domains from smart cities and agriculture to industry and medicine. At the heart of this expansive reach is the Internet of Things (IoT), poised to interlink billions of devices with the traditional Internet. Many of these devices, while cost-effective, come with inherent constraints related to energy, computation, storage, and communication capabilities. The overarching success of IoT hangs on these resource-limited objects’ ability to operate reliably and sustainably while maintaining connectivity [1].

In IoT systems, energy efficiency stands at the forefront of technological challenges, with researchers globally striving

Ahlam Hannachi and Salim Bitam are with the Department of Computer Science, University of Biskra, Biskra, Algeria (e-mail: ahlam.hannachi@univ-biskra.dz; s.bitam@univ-biskra.dz).

Wael Jaafar is with the Department of Software and IT Engineering, École de Technologie Supérieure (ETS), Montreal, Canada (e-mail: wael.jaafar@etsmtl.ca).

Nabil Ouazene is with the Laboratory of Applications of Mathematics to Computing and Electronics, University of Batna 2, Batna, Algeria (e-mail: nabil.ouazene@univ-batna2.dz).

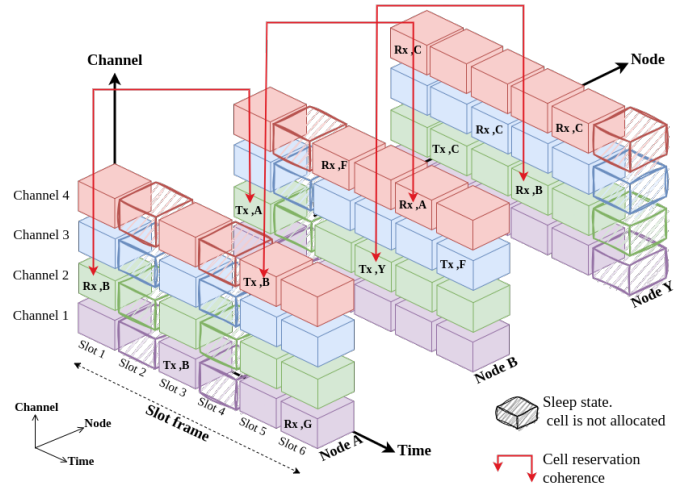


Fig. 1: TSCH schedule of nodes A, B, and Y.

to meld enhanced performances with reduced or equilibrated energy consumption. Specifically, the medium access control (MAC) layer is pivotal in controlling the energy drain since it ensures the network’s reliability by regulating access to the shared communication medium; typically a wireless channel. The IEEE.802.15.4e standard has been crafted to cater to industrial applications. It introduces different operational MAC modes, such as Time Slotted Channel Hopping (TSCH), Deterministic and Synchronous Multi-channel Extension (DSME), and Low Latency Deterministic Network (LLDN) [2], [3]. Among these modes, TSCH stands out as the leading one and is included in several standards such as ANSI/ISA100.11a and WirelessHart IEC62591 [4], [5].

The core concept of TSCH lies in the integration of Time Division Multiple Access (TDMA) with channel hopping techniques. This fusion results in a dual medium access mechanism based on time and channel. In this context, “time” is referred to by *time slot*, and “frequency” is referred to by *channel*. A time slot within a specific channel is defined as a *cell*. For every time slot, shown in Fig. 1, an IoT node specifies its activity in a given channel, choosing to transmit to a node (Tx), receive from a node (Rx), or sleep, with the latter not requiring any specific cell selection [6]. The efficiency of the TSCH schedule is reflected in the consistent actions of devices. Thus, each device has to judiciously select the combination of (state, cell, neighbor), where the $state \in \{Tx, Rx, Sleep\}$. For instance, in node A’s TSCH schedule in Fig. 1, the cell (*slot 1, channel 2*) is set for receiving from node B. Conversely, in node B’s schedule, the same cell is allocated for transmitting to node A. Moreover, A is set to sleep mode during time slots

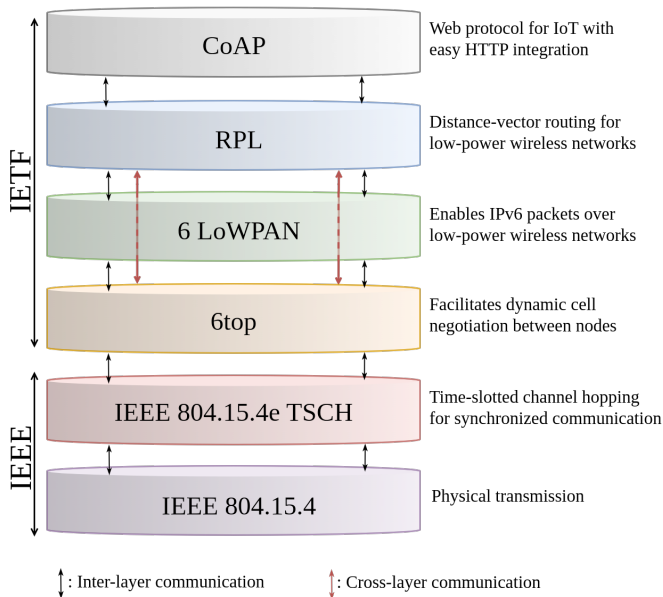


Fig. 2: The 6TiSCH protocol stack (Adapted from [9])

2 and 4, while B enters sleep mode in time slot 2.

As the transition from IPv4 to IPv6 becomes more pressing due to IPv4's address limitations and IPv6's advanced capabilities, compatibility issues have risen. To tackle them, several bridging technologies have been developed to cope with the protocols' distinct structures and behaviors. The latter became the *de facto* tools of the protocols' coexistence, and thus ensuring a smooth transition from IPv4 towards IPv6. Within this framework, the Internet Engineering Task Force (IETF) took the initiative of forming the 6TiSCH working group, aiming to establish protocols that facilitate the implementation of IPv6 over the TSCH mode. The proposed protocol stack is depicted in Fig. 2. Specifically, the 6top layer holds the Scheduling Function (SF) responsible for TSCH cell allocation and traffic demands/performance metrics monitoring. The conventional SF is the Minimal Scheduling Function (MSF) [7].

Moreover, the Routing Protocol for Low-Power and Lossy Networks (RPL) layer, which encompasses the Objective Function (OF), plays a pivotal role in establishing and sustaining the routing topology. It does so by constructing a Destination-Oriented Directed Acyclic Graph (DODAG), a structured network topology that enables optimized routing. Through DODAG, RPL efficiently propagates routing information, tailoring pathways based on various critical metrics to meet the specific demands of the network. This mechanism is fundamental in addressing the complex routing challenges inherent in low-power and lossy networks, particularly within the Industrial IoT (IIoT) framework. The latter allows IoT nodes to discover their best potential parents and establish a route towards the network root. The conventional OF of RPL is the Objective Function Zero (OF0) [8].

Both RPL and 6top utilize control packets to maintain and optimize the IoT network's operation, namely DODAG Information Solicitation (DIS), DODAG Information Object (DIO), and Destination Advertisement Object (DAO) for RPL,

and 6P transactions in 6top. The relation between RPL and 6top is reciprocal. For instance, while RPL alters the routing topology by changing a node's parent, 6top dynamically adjusts the scheduled cells to accommodate this change, i.e., releasing assigned cells to the old parent and negotiating new cell allocation with the new parent. RPL determines the next-hop parent for data transmission based on its topology, while 6top ensures cell availability for this specific transmission according to the TSCH schedule.

However, this cross-layer interaction between the RPL and 6top layers (shown by red lines in Fig.2) controls implicitly very critical performance factors. To the best of our knowledge, very few works have investigated the nature of this interaction. Consequently, we propose a novel approach that improves the RPL-6top interaction, while aiming to reduce energy consumption and enhance the spatial reuse of resources. Our contributions can be summarized as follows:

- We aim to reduce the number of control packets by merging two types of control packets and to simplify the cell negotiation and assignment process. Specifically, upon parent switching, RPL control messages will be used for cell allocation rather than transmitting separate 6P transaction messages.
- We eliminate instances of parent switching failures, prevalent when the new parent schedule is at full capacity. This is achieved by embedding a list of available slots within the DODAG Information Object (DIO) packets. Consequently, a transition to a parent offering a superior rank will only be executed if the list of its free slots satisfies the requirement of the new child.
- We improve the jitter and latency by adopting proximity-based slot selection rather than the conventional random selection.
- To preempt packet drop events that occur when the TSCH queue reaches its limit, we propose setting a predefined queue size to solicit new cells from the parent node.
- Through extensive simulations over the 6TiSCH simulator, we prove the superior performance of our proposed method in terms of joining time, energy consumption, traffic load, delivery ratio, and jitter, compared to the MSF benchmark.

The structure of this paper is outlined as follows: Section II presents a comprehensive overview of the research context and discusses related works. Section III delves into the intricate details of the proposed solution. Through simulations, section IV evaluates the performances of our approach and compares them to those of the MSF benchmark. Finally, Section V concludes the paper.

II. CONTEXT AND RELATED WORK

In the field of 6TiSCH networks, ongoing research is dedicated to developing effective, reliable, and energy-efficient communication strategies. This often involves examining and refining existing standards. In this section, we first outline the key conventional protocols within the 6TiSCH stack, thus providing the foundational framework for researchers. Then, we highlight recent related works.

A. Context: 6TiSCH Background

The 6TiSCH standards lay the groundwork for the operation of IIoT networks. We present their main components relevant to our research, namely the Minimal Configuration (MC) and the Minimal Scheduling Function (MSF). The MC details the procedure for the node joining process [10], while the MSF defines the scheduling mechanism, which outlines how communication cells are assigned and released [11].

1) *Minimal Configuration*: The MC defines the sequential steps that each node must undertake before becoming operative and start transmitting data. Its steps, shown in Fig. 3, are described as follows:

- *Synchronization*: Initially, each node is in a “pledge” state, passively listening on randomly selected channels to anticipate Enhanced Beacons (EBs) sent by nodes that are already part of the network, including the root node that initiate the network formation. Upon the reception of a predefined number (nb) of EB packets, a pledge synchronizes with the IoT network. For instance, node A in Fig. 3 starts as a “pledge” at time T and synchronizes at time T_{Sync}^A , where energy is expended inefficiently during the interval $T_1 = T_{\text{Sync}}^A - T$.
- *DODAG joining*: After synchronization, if secure joining is required, the node sends a “JOIN REQUEST” to the EB source and awaits the “JOIN RESPONSE”. Otherwise, it directly sends a DODAG Information Solicitation (DIS) packet. The DIS mechanism operates in two distinct modes:
 - *Unicast DIS*: In this mode, the receipt of a DIS message prompts the targeted node to respond with a DIO message.
 - *Broadcast DIS*: In this mode, receiving a DIS message leads nodes to reset their DIO trickle timers, thereby influencing the timing of subsequent DIO message dissemination.

The DODAG joining is driven by the periodic multicasting of DIO messages by nodes that have previously integrated the DODAG. DIO messages encapsulate vital information regarding the DODAG, including its identification (ID), version, and the node’s rank within the structure. DIO packets are delineated into:

- *Periodic DIO*: These messages are needed to establish and sustain the topology of a DODAG. They provide critical information about the DODAG’s configuration, including the sender’s rank and set of nodes utilized for parent selection within the DODAG. The period of the DIO transmission is defined by the Trickle algorithm, and according to the network’s consistency [12].
- *DIO as a response*: It is a unicast response to a DIS packet sent by a soliciting node asking for relevant routing information. For instance, node A in Fig. 3 joins the DODAG at time T_{Join}^A , where the time interval $T_2 = T_{\text{Join}}^A - T_{\text{Sync}}^A$ corresponds to the joining procedure.
- *Cell allocation*: Once synchronized, every node reserves its first cell, referred to as the “minimal cell”, at time slot 0 and channel 0. Following this initial reservation, when a

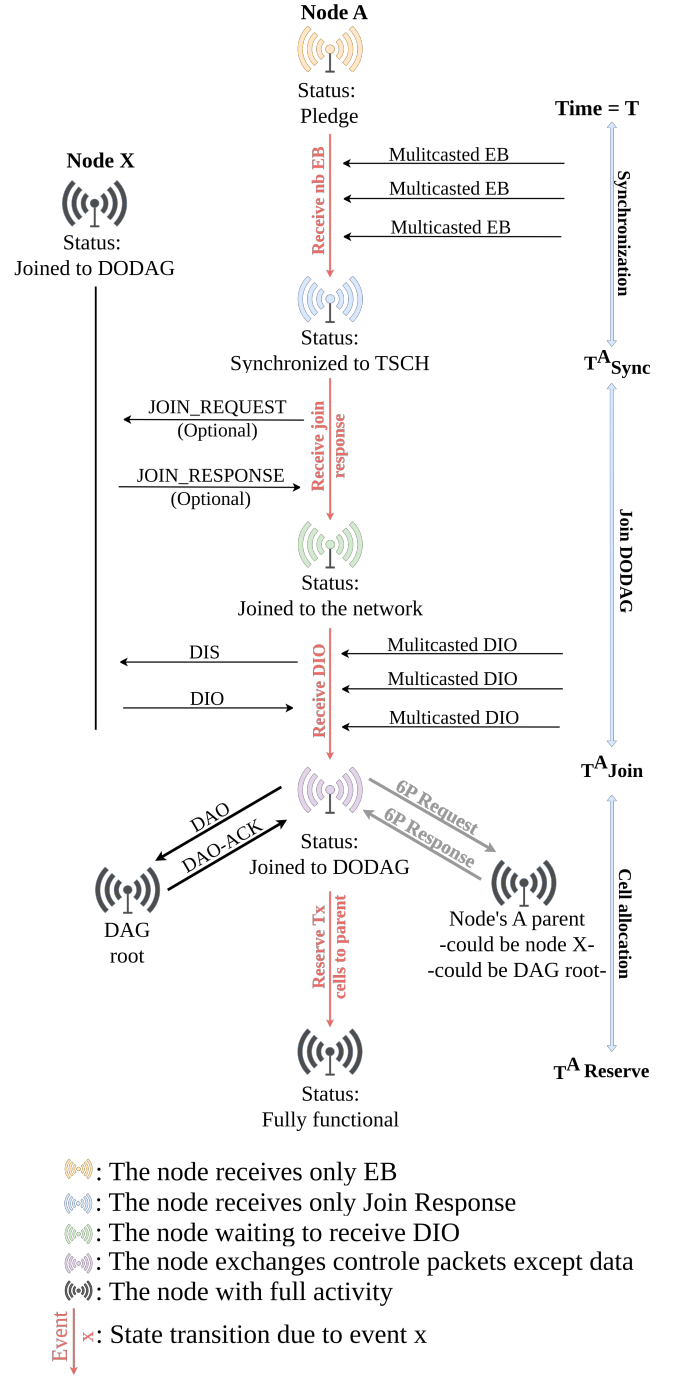


Fig. 3: 6TiSCH network formation (MC).

node receives a DIO message, it selects a parent among neighbors that advertised the DIO messages, according to the RPL’s objective function. Then, the node triggers the process of cell reservation with the new parent by initiating a 6P transaction and transmits a DAO packet to the DAG root to indicate its parent, so that the DAG root can build/update the topology tree. If the parent is the DAG root itself, then the node sends both the 6P transaction and DAO packet to it. DAO packets are destined to the DAG root to facilitate the update of the routing tree. They come in two types:

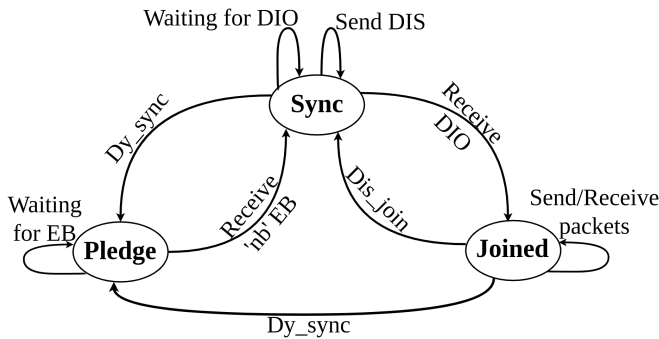


Fig. 4: Node status cycle.

- *Periodic DAO*: It is transmitted periodically and used to maintain and refresh the route information at the DAG root.
- *Parent Switching DAO*: It is sent immediately after a parent-switching event to swiftly notify the DAG root of changes in the routing topology.

In summary, nodes within 6TiSCH networks dynamically alter their operational states throughout their life cycle, influenced by localized parameters and network conditions. These transitions and state changes, illustrated in Fig. 4, embody the node’s continual attempt to preserve network connectivity, synchronization, and data transmission integrity within the inherently challenging communication environment of 6TiSCH networks. Notably, a node reverts to its initial “pledge” state if it fails to receive any packet within a predefined temporal window (Dy_sync), indicative of potential communication disruptions or isolation from the network. Furthermore, if the node experiences a linkage failure to its parent or while executing parent switching (Dis_join), it regresses to a “synchronized” state, reflecting a lack of association with the DODAG, yet maintaining synchronization with the network’s time source.

2) *Scheduling Function*: The scheduling function, SF, serves as a critical mechanism to allocate time slots and channels within the TSCH mode. Its primary role is to manage the scheduling of communications across the time-frequency domain. By dynamically responding to the varying demands and conditions of the network, SF ensures the judicious use of resources and maintains dependable communications. As shown in Fig. 5, the SF conducts the cell reservation procedure using 6P protocol transactions [11], [13], where the term “Requester” denotes a node in need of reserving new cells from another node, referred to as the “Responder”. In this process, the “Requester” initiates the cell reservation process. There are two distinct approaches: the 2-step and 3-step methods. The key difference lies in which node proposes the list of cells. In the 2-step transaction illustrated in Fig. 5a, the “Requester” proposes the list of cells, which leads to exchanging two control packets, whereas in the 3-step transaction, presented in Fig. 5b, the “Responder” proposes the list of cells, thus exchanging three control packets. Nevertheless, in both approaches, the proposed cells are locked during the period T_{Lock} .

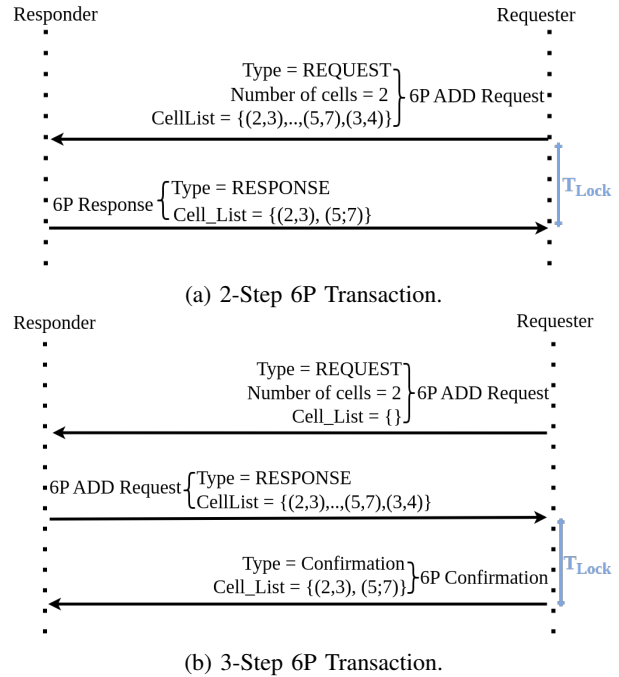


Fig. 5: An Example of 6P Transactions.

The conventional SF of the 6TiSCH protocol stack is the Minimal Scheduling Function, which follows a strategy of random cell selection, both in cell proposal during 6P transactions and in cell reservation among the proposed/available cells. Nevertheless, the nodes dynamically determine the number of cells needed based on their traffic requirements and network conditions. Although this stochastic approach provides adaptability to varying traffic conditions, it may face challenges such as internal collisions, particularly in dense networks. This raises concerns about its applicability in scenarios with stringent Quality-of-Service (QoS) requirements.

B. Related Works

The conventional mechanisms, while foundational, have been scrutinized for potential limitations and areas of enhancement. This section investigates the existing literature for proposed methodologies, achievements, and gaps, thereby contextualizing the motivation and novelty for our work.

Aiming to enhance fundamental aspects of 6TiSCH, in particular the TSCH configuration, authors of [14] adopted heterogeneous time slot length in MSF to minimize communication latency. In [15], the authors introduced a heuristic for parent selection in multi-PHY TSCH, showing that slot bonding can adapt to different PHY data rates and achieve high Packet Delivery Ratios (PDRs).

From the perspective of network formation in 6TiSCH, the study conducted in [16] evaluated the network formation procedure, and pinpointed numerous limitations within its scope. Then, they proffered several recommendations and established guidelines for parameter adjustments, tailoring them to several network topologies. Also, authors of [17] addressed performance degradation during 6TiSCH network formation. They highlighted the challenges faced by new nodes joining

the network, primarily due to the policy of allocating only one shared cell per slotframe for control packet transmission. They particularly emphasized the limitations of prioritizing EBs during network formation. Then, they proposed an improved approach that effectively integrates control packets into the network formation process.

Typically, research works that enhance SF fall into three categories: 1) Centralized approaches such as [18], [19], 2) distributed approaches like [20], and 3) autonomous approaches, e.g., [21]. In [18], the authors proposed a fully centralized schedule for data gathering, where each node has to send the allocation request to the DAG root and receive the answer, thus wasting a considerable amount of energy and time. Alternatively, in [19], a central entity is responsible for managing the scheduling of transmissions in the network and uses a recurrent neural network (RNN) based model to predict the next transmission slot for each node, aiming to reduce the latency of end-to-end communications. However, a higher control packets overhead is generated. Moreover, authors of [22] introduced an Adaptive Static Scheduling (ASS) technique designed to enhance the network’s energy efficiency. Several works delved into the scheduling strategies and network formation solutions. They are comprehensively summarized in surveys, e.g., [23], [24]

Other works focused on optimizing the RPL’s objective function. For instance, authors of [25] introduced a novel parent selection function that accounts for the number of neighbors and traffic load and aiming to optimize the PDR, while minimizing frequent parent switching. In [26], a Q-learning based algorithm is proposed to refine the RPL’s objective function, while [27] proposed an early parent switching scheme, based on the remaining queue capacity of the parent node. Finally, the study in [27] introduced a novel parent switching scheme predicated on the remaining queue capacity of the parent node, which effectively improved the PDR performance.

III. PROPOSED SOLUTION

Our work extensively focus on the intricate interplay between RPL and SF, and between SF and packet queue management. The core philosophy of our solution is as follows: 1) Reduce the transmission frequency of control packets upon parent switching; 2) Minimize the number of failed parent switching events that result from cell unavailability; 3) Prevent packet dropping events due to queue saturation; and 4) Improve the jitter and latency performances by slot selection. Our approach targets saving valuable energy resources and mitigating unnecessary medium contention, thus enhancing the spatial reuse.

For understanding purposes of our solution, we highlight the following technical terms usage:

- Reference to “DAO” is explicitly linked to the DAO packet triggered upon parent switching, unless otherwise specified. This specificity arises from our focus on mechanisms and enhancements relevant to the parent-switching events, while the processes involving periodic DAO packets remain unaltered through our approach.

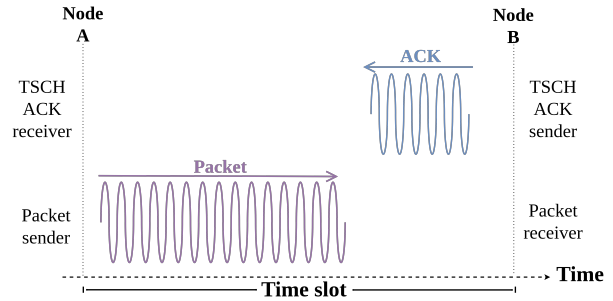


Fig. 6: Packet TSCH Acknowledgment.

- Reference to “DIO” may refer to either periodic or direct response to a DIS packet, dependent on the context of the mentioned processes or mechanisms.
- “DAO-ACK” and “ACK” are two distinct message. DAO-ACK denotes a packet transmitted by the DAG root during a to acknowledge DAO messages for reliable route registration/de-registration. In contrast, a packet “ACK”, known also as a link-layer or TSCH acknowledgment (shown in Fig. 6), is issued upon packet reception [28].

A. Regulated Triggering of Parent Switching

In 6TiSCH networks, parent switching might be challenging. Indeed, the decision to switch to a potentially superior parent is complex, given the node’s lack of awareness regarding the new parent’s cell availability. This uncertainty can lead to inefficient energy usage since the node may continue control packet transmissions without realizing effective cell allocation. Also, the RPL specifications [8], [29] did not detail the protocol’s behavior regarding transmission interruption to the former parent during this process. Consequently, increased latency and potential packet loss may occur. To tackle this issue, our solution proposes to modify the DIO packet in order to carry a list of available slots of the sender. This approach ensures that a node initiates parent switching only when a shared available slot exists, hence improving the efficiency of the process. Algo. 1 below delineates this mechanism, particularly focusing on the node’s decision-making process at the juncture of parent switching.

B. Minimizing 6P Transaction Packets

In the sequenced control packet transmission process of 6TiSCH networks, depicted in Fig. 3, when a node decides to change its parent, it communicates this transition by transmitting a DAO packet to the DAG root and triggers the cell reservation process with the new parent. This entails dispatching a cell reservation request using a 6P transaction as shown in Fig 5.

Rather than dedicating an entire packet for this purpose, we propose to judiciously embed the requisite information for cell reservation within the RPL control packet DAO. Since the next hop for each child packet is inherently its parent, all packets, including the modified DAO, will go through the designated parent and hence can extract the embedded information about

Algorithm 1: Parent switching procedure

```

Data: parents : DIO's senders
         min_nb: Minimum number of slots to allocate
         max_nb: Maximum number of slots to allocate
Result: Parent switching decision
         nb : Number of slots to reserve

// ----- Initialization
1 nb_parentSlot ← Number of slots allocated to parent
2 child_slots ← Node's free slots

// ----- Parent Selection and Slot Reservation
3 selected_parent ← parent | parent.rank =
   min(p.rank For p in parents and p.free_slot ∩ child_slots ≠
   ∅)
4 if selected_parent ≠ None then
5   if Old parent is None then
6     // Node is joining the DODAG
7     nb ← min_nb
8   else
9     // Node is switching parent
10    nb ← nb_parentSlot
11    if nb > max_nb then
12      // Ensure selected slots are not
13      // exceeding the max limit
14      nb ← max_nb
15    free_slots ← child_slots ∩ parent_free_slots
16    slots ← Select nearest nb slots from free_slots
17    child_slots ← child_slots − slots
18    Append slots to DAO packet
19    Append child_slots to DAO packet
20    Transmit DAO packet
21 else
22   Pass
23   // Retain current situation since there is
24   // no slot availability

```

cell reservation and define its relevant cells. This approach is detailed as follows:

- 1) *Autonomous channel selection*: Transmission channel is autonomously determined based on the MAC address of the receiver, thereby enabling nodes to distribute only the slot offset to represent the cell. To avoid interference and benefit from multi-channeling, we adopt the same approach as MSF. Specifically, the current transmission/reception channel (*channel_ID*) is determined based on the Absolute Slot Number (ASN) and the channel offset (*cell_{channel}*) of the current cell as follows:

$$channel_ID = (ASN + cell_{channel}) \% nb_channels, \quad (1)$$

where $nb_{channels}$ is the total number of channels and $\%$ is the remainder of the Euclidean division.

- 2) *RPL packet size management*: In 6TiSCH networks where the packet size is intrinsically constrained, judicious management of the RPL packets DIO, DAO, and DAO ACK, is important. Consequently, we propose the following modifications:

- a) *Selective data injection*: Conventionally, cells are represented as tuples of slot-offset and channel-offset. Their injection into the RPL packets leads to increased packet size and processing time. Aiming to reduce packets' size, we propose a simplified integer-only representation of the available cells instead of using

space-greedy tuples.

- b) *Efficient Slot ID encoding*: To further enhance the packet size, we introduce an encoding scheme for slot IDs. Typically, 6TiSCH systems limit the slotframe length to 101 slots. However, we propose here to extend the slotframe length to 255 slots, such that the slot ID never exceeds this value. By doing so, we can encode each slot ID into a single byte (8 bits), thus minimizing the slot ID data size injected into the packet.
- c) *Compact free slots notation*: Within our proposed approach, the DAO and DIO packets have to convey the node's free slots. To optimize memory usage, we propose that the node transmits either an ordered list of occupied slots or of free slots, depending on which is shorter and anticipating it with a flag (1 bit). Within the 6TiSCH context, slot "0" is reserved by nodes upon joining the network, hence it will never be included in the ordered list of free slots. This reserved status allows to efficiently utilize slot "0" as the flag for the occupied/free slots list. This flexible method guarantees less memory usage.

The aforementioned techniques align with the fundamental requirements of low-power and lossy networks (LLNs) since they aim to reduce transmission overhead, save energy, and enhance the network's throughput. Moreover, they simplify demands' processing, which is critical for devices operating within constrained environments, such as in 6TiSCH networks.

- 3) *TSCH ACK-based optimization of slot allocation*: For efficient time slot allocation, we propose a novel method that uses TSCH ACK for immediate confirmation of slot reservations upon DAO packet reception. Doing so bypasses the conventionally incurred delays for reservation confirmation. Leveraging TSCH ACK ensures quicker communication of available time slots, thus reducing the locking duration of time slots (shown as T_{Lock} in Fig. 5) and increasing the network's flexibility for topological changes. Our technique embeds a list of available slots (identified with integers) directly into the TSCH ACK messages. For the sake of data size reduction, we limit the maximum number of time slots allocated at once to 5 resulting in an additional payload of merely 5 bytes in TSCH ACK. Moreover, to ensure efficient time slot reservation, we assume that each node maintains an up-to-date variable containing its ordered available slots list. This variable is dynamically updated following each slot allocation or de-allocation. Upon receiving a packet, the joining node compares the list of available slots embedded within the packet against its variable of available slots. Hence, the decision to reserve slots is based on the most current network status, which improves the responsiveness and adaptability of the 6TiSCH network to real-time demands.

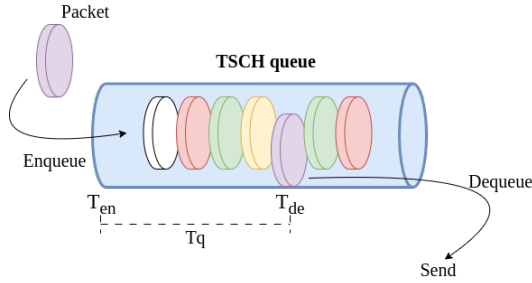


Fig. 7: Illustration of a packet time in a 6TiSCH queue.

C. Reducing DODAG Joining Time

To reduce packet collisions and reduce the nodes' joining time, we propose that the DIO sender sets temporary time slots or cells, ensuring it is actively listening, and it designates one permanent cell to maintain its ongoing listening state. In scenarios where a DIO is concurrently received by multiple nodes, thus causing potential DAO collisions, the proposed mechanism that uses a combination of temporary and permanent cells can diminish the impact of this issue as follows: 1) The DAO sender temporarily allocates cells until it receives the TSCH ACK of the DAO packet. This strategy intentionally sacrifices idle listening to prioritize energy saving, given that the energy consumed during idle states is notably lower than that needed to manage collisions and trigger packet retransmissions [30]. 2) In the initial phase of network formation where nodes actively compete to join the network and parent switching events are frequent, our method sets a high number of proposed time slots in the DIO to facilitate rapid integration and reduced collision events. As the network stabilizes, we strategically reduce the number of proposed slots to preserve energy.

D. Scheduling Information Injection

In the context of TSCH, transmitting packets from higher-layer protocols is not an instantaneous process; rather, it entails a meticulous queuing and scheduling mechanism. As depicted in Fig. 7, incoming packets are first enqueued within the TSCH queue and await their transmissions. Since we inject the proposed time slots in DIO and DAO packets, they will be locked during time $T_q = T_{de} - T_{en}$, where T_{en} is the instant at which the packet entered the TSCH queue, and T_{de} is the time at which it left the queue. To avoid locking the proposed time slots for a long time T_q , we propose to inject them within the packet only before leaving the queue, i.e., at instant T_{de} , hence $T_q \approx 0$. By carefully orchestrating the data injection in the RPL control packets, we optimize time slot utilization.

E. Avoiding TSCH Queue Overflow

In 6TiSCH networks, effective synchronization between SF and TSCH queue management is essential for network operation. With various protocols filling the queue with packets, timely processing during the SF-designated transmission cells is crucial. A mismatch between the queue and cell allocation can lead to packet loss. To address this issue, we propose the

TABLE I: Simulation parameters

Parameters	Value
Number of nodes	50, 100
Number of simulation runs	100
Simulation duration (min)	30, 270
Network area (km ²)	1
Service or application packet period (sec)	5, 15, 45, 60
Slotframe length (in number of slots)	100
Time slot duration (sec)	0.01
Secure Joining required	True
TSCH maximum payload length (bytes)	120
TSCH queue size (number of packets)	10
DIO packet size (bytes)	MSF PB
	76 120
DAO packet size (bytes)	20 75

introduction of an early cell reservation technique. Specifically, as the TSCH queue begins to be filled and before reaching its limit, our system proactively initiates 6P transactions with the preferred parent for an additional cell reservation. This proactive approach offers several benefits: 1) *Prevent packet drops*: Early reservation of additional cells reduces the likelihood of packet loss due to queue overflow, and 2) *Mitigate resource urgency*: This method allows nodes to secure necessary resources in advance, thus avoiding the last-minute pressure of queue overflow and network instability.

F. Adaptive Self-Sufficient Cell Reservation

In a typical 6TiSCH network, all DAO packets are destined towards the DAG root, thus navigating in a multi-hop fashion. In our proposal, essential information about cell reservation, which consists of the available slots and proposed slot lists, is embedded within these DAO packets. When a parent node receives a DAO packet, as it is the principal conduit to the DAG root, it reserves new cells for its new child where the number of cells should not exceed the maximum number of cells to allocate at once. Then, it loads the list of its free slots (instead of the old one that belongs to the child) and the number of slots to be selected (slots to be allocated to its new child) into the DAO packet. This packet is then seamlessly forwarded, with each intermediate node towards the DAG root executing the same procedure. As shown in Fig. 8, upon reception of a DAO packet from node 3, node i undertakes cell selection for reservation and embeds the list of chosen slots into the TSCH ACK packet. It then forwards the enhanced packet to its parent. To reduce latency at every hop, we propose that the receiver of a DAO packet selects the nearest time slot to the actual one used for the reception. One way to do it is to rely on the concept of the Low-Latency SF (LLSF) protocol [31] where the slots are selected according to the gap to the left of the actual slot. However, we propose here to select the nearest slot to the actual one in any direction. Accordingly, if the node is joining the DODAG, the actual slot will be in the list of proposed slots, thus maximizing its chance of selection. If the node has already joined the DODAG, then the actual slot is the slot that is already allocated to its parent. Consequently, both energy and latency tied to time slot reservations can be reduced.

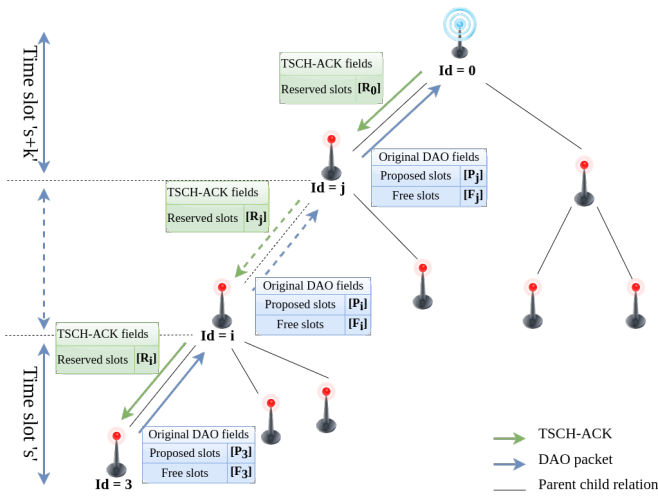


Fig. 8: Illustration of the DAO packet transmission and TSCH ACK utilization.

IV. PERFORMANCE EVALUATION

A. Simulation configuration

To comprehensively assess the efficiency and resilience of our proposed scheme, we employed the 6TiSCH simulator [32]. For the sake of thorough analysis, generated plots include outlier results, thus reflecting the full range of observed results. Our simulations spanned 30 minutes and 270 minutes (4.5 hours) and were repeated 100 times across two distinct network configurations:

- *Conventional 6TiSCH configuration:* It consists of the use of the conventional MSF as the scheduling function and OF0 as the RPL objective function [8], [11]. Within the results, this configuration is denoted as “MSF”.
- *Proposed solution-based configuration:* This setup leveraged our proposed solution with the modified MSF and OF0 as the scheduling and objective functions, respectively, and labeled as “PB” within the results.

For our simulations, we assume a 1×1 km² area, where $N = 50$ or $N = 100$ nodes are randomly deployed [32]. Moreover, we assume that the frequency of data transmissions for the application or service is in the values $\{5, 15, 45, 60\}$ seconds. Also, the slotframe length has been fixed for all nodes in the network, either equal to N or to $2N$. The remaining simulation parameters are presented in Table I, while Table II exposes the specific parameters of the proposed solution.

The selected value for the “TSCH queue empty places threshold for cell reservation” is justified as follows. Upon each packet enqueueing operation, nodes assess the remaining capacity within the TSCH queue. When the available space in the queue reaches a predefined threshold, the node initiates a cell reservation request using the 6P protocol, where “Number of cells reserved upon reservation process” (specified in Table II) cells can be requested at that time, and subsequent requests will be constrained by the value of the parameter “Cycle interval before next cell request”. This threshold is set to 2 empty places in the queue to accommodate the 6P transaction packet and to reserve capacity for any imminent packet. Such

TABLE II: Parameters of the proposed solution

Parameter	Value
Number of proposed slots per DIO	7
DIO cells duration (in number of slotframes)	10
Number of permanent DIO slots	1
Slot selection ratio within DIO slots	3
Maximum number of cells to reserve at once	5
Initial phase duration (min)	45
TSCH queue empty places threshold for cell reservation	2
Cycle interval before next cell request	2
Number of cells reserved upon reservation process	1

a configuration prevents queue overflow and enhances the network’s capability to handle data packets, especially in dense-traffic scenarios.

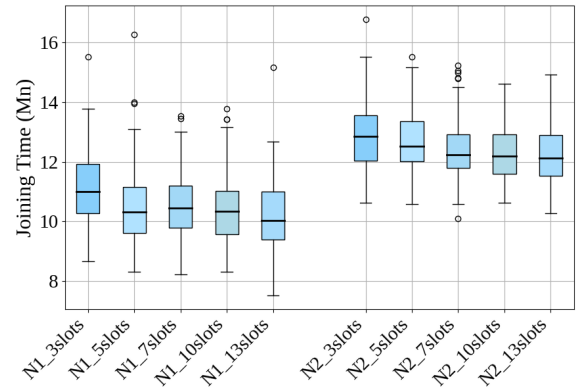


Fig. 9: Joining time vs. nbr. of proposed slots per DIO.

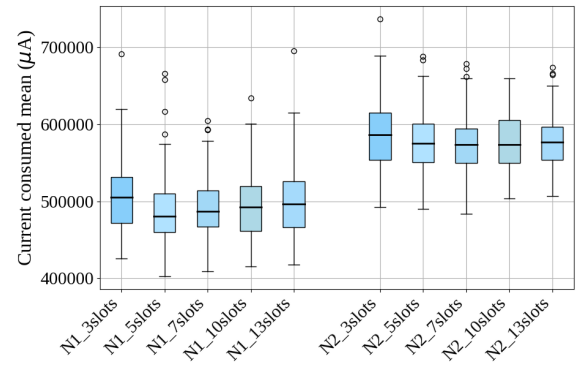
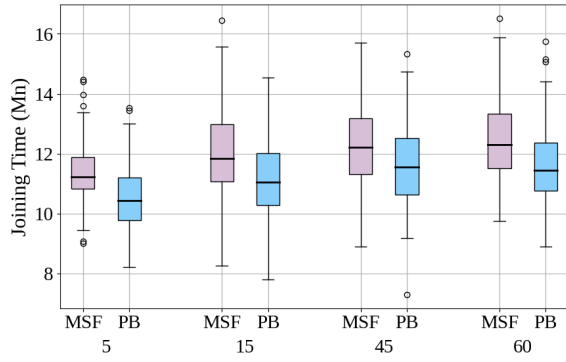


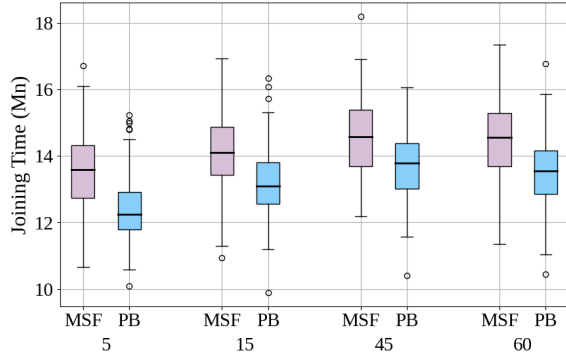
Fig. 10: Consumed current vs. nbr. of proposed slots per DIO.

To set the parameter “Number of proposed slots per DIO” in Table II to the best value, we conducted several experiments with different values. Specifically, in Figs. 9-10, we evaluated the impact of different numbers of proposed time slots per DIO on the joining time and current consumption (equivalent to energy consumption).

These experiments have been conducted over an observation time of 30 minutes, with an application period of 5 seconds, and for different network sizes, i.e., $N_1 = 50$ and $N_2 = 100$ nodes. As shown in Fig. 9, for any number of nodes, the



(a) $N = 50$



(b) $N = 100$

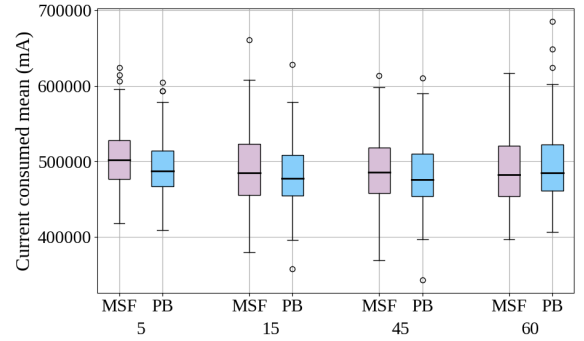
Fig. 11: Joining time vs. length of service packet period (in sec) (first 30 minutes).

joining time reduces when the number of proposed slots is higher. This is expected since more proposed slots mean that a novel node can rapidly be configured and join the DODAG. However, since the number of proposed slots cannot be very high, as it may increase the size of packets, our preference is for the value 7 since it provides similar results to the system with the value 13, in particular for N_2 , i.e., for a large network. A similar explanation can be provided for Fig. 10 where the value 7 achieves low current consumption for the large network. Indeed, a very high value, such as 13, can result in inefficient idle listening, thus increasing power consumption. Consequently, we recommend the number of proposed slots per DIO to be 7 as the best value since it is the lowest one that achieves good performances in terms of joining time and consumed power.

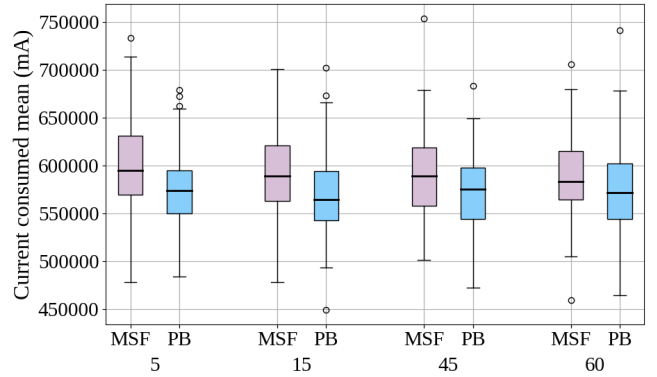
B. Simulation Results

The initial phase of the network’s life is known as network formation. This phase is pivotal for establishing the network’s parameters and topology. To demonstrate the effectiveness of our solution in accelerating the network formation timeline and minimizing power consumption [30], we conducted simulations in Figs. 11-12 under the same conditions as the previous figures, while we varied the value of the parameter “Service packet period”. Also, we compared the results of our proposal, denoted PB, with those of the benchmark MSF.

As shown in Fig 11, our proposed solution PB achieves lower joining time for any N and service packet period



(a) $N = 50$



(b) $N = 100$

Fig. 12: Consumed current vs. length of service packet period (in sec) (first 30 minutes).

duration. For instance, PB achieves an average joining time of 13 minutes for a service packet period equal to 15 and $N = 100$, while MSF needs approximately 14 minutes in the same conditions. Indeed, a node within the PB framework uses proposed slots in the received DIO to define the cells during which it sends the DAO, unlike MSF which relies on sending a 6P request to its preferred parent and then waiting for a response for cell reservation. In PB, the DAO packet serves a dual purpose: Communicating with the RPL to establish the DODAG structure and participating in SF. As the service packet period increases, we notice a degradation in the joining time. This is expected since a node with a low (resp. high) service packet period will transmit EB packets more (resp. less) often, which increases (resp. reduces) the likelihood that other nodes synchronize and join the DODAG.

In 6TiSCH networks, the process of network formation often expends a significant amount of energy, even before useful data transmission. In Fig. 12, we present the consumed current related to the scenarios of Fig.11. The PB scheme performs better than the MSF one, for any N and service packet period duration. The performance gap increases as N becomes higher. This result proves the robustness of our scheme and its superiority when operating in dense networks. Finally, we notice that the service packet period has a slight impact on the total consumed current.

After validating the improvements of our solution on network formation, we assess the performances of the schemes for long-term operation. We evaluate the performances in terms

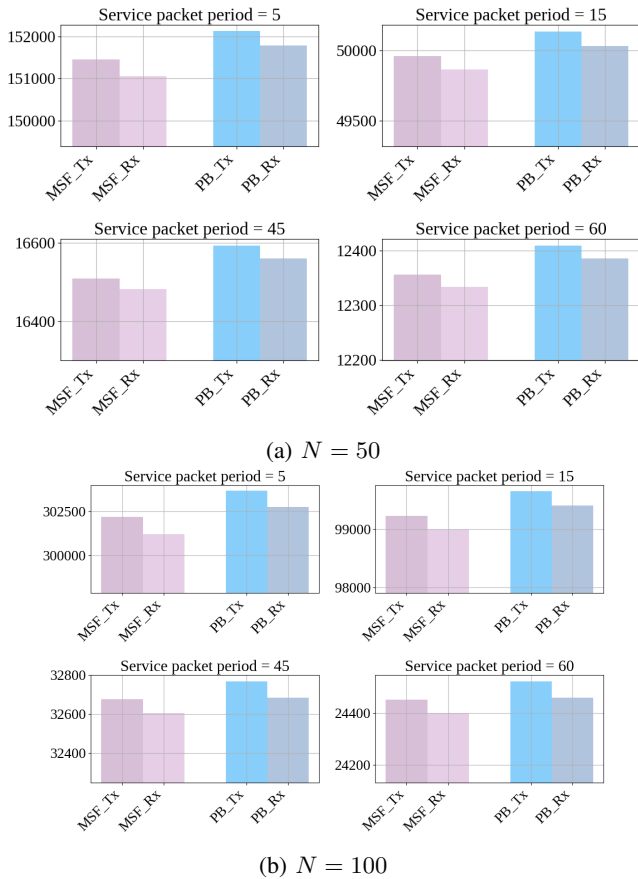


Fig. 13: Total nbr. of sent/received packets (different service packet periods, 4.5 hours).

of the number of packets transmitted/received, the end-to-end (E2E) latency, network jitter, and consumed charge. For the next results, experiments have been conducted for 4.5 hours.

Fig. 13 illustrates the number of transmitted (Tx) and received (Rx) packets for different service packet periods and N , where PB and MSF are compared. For any N and service packet period, our solution outperforms the MSF benchmark. In other words, the network that uses our approach realizes more frequent transmissions, and nodes within it successfully receive more packets. When the service packet period increases, i.e., a longer service is running, the number of exchanged packets drops. Such a result is expected since during the observation time of 4.5 hours, a longer service time impacts the frequency of its execution over the observation period. Moreover, when $N = 100$, the number of exchanged packets almost doubles compared to the case with $N = 50$. Indeed, the availability of more nodes joining the DODAG makes it possible to transmit/receive more packets, within the limits of available channels and time slots in 6TiSCH.

Fig. 14 shows the network's E2E latency for different service packet periods and N . End-to-end latency is defined as the duration measured from the ASN at which a source node transmits a service/application packet, to the ASN at which this packet is successfully received and acknowledged by the destination. As it can be seen, the PB scheme achieves lower E2E latency in any network condition than the MSF benchmark.

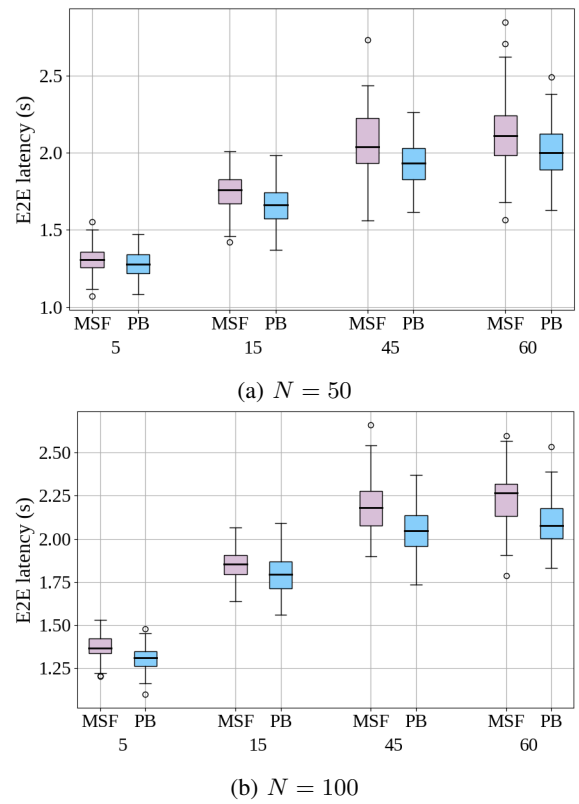


Fig. 14: E2E latency vs. service packet period (in sec) (4.5 hours).

This result underscores the efficiency of our method. Even when the service packet period increases, the E2E latency follows in a logarithmic trend with values stabilizing at high values. For instance, for $N = 100$, the average E2E latency is almost the same, about 2.1 sec, for service packet periods 45 and 60.

In Fig. 15, we plot the median and average jitter performance for the transmitted packets during the observation time, for different N and service packet periods. Jitter refers to the variation in packet transmission latency over time within a network. It is the inconsistency observed in the arrival time of packets, primarily caused by varying network congestion levels, route changes, or other unforeseen factors. To obtain the median and average results, we generated 100 scenarios for each packet order point. The median offers insight into the typical experience of a node without the influence of outliers, while the average jitter aggregates these variations to provide a general sense of the network's jitter over time. According to Fig. 15, MSF shows an initial peak (median and average jitters), due to the network's formation phase, which might disrupt real-time services. In contrast, PB consistently maintains lower jitter performances than MSF, which indicates a stable packet delivery time. The median jitter of MSF exhibits high variability, thus unsuitable for services requiring consistent data rates, while PB follows a more predictable jitter performance, which makes it fit for real-time applications. As N increases from 50 to 100, and for a given scheme and service packet period, we notice that the jitter performance is

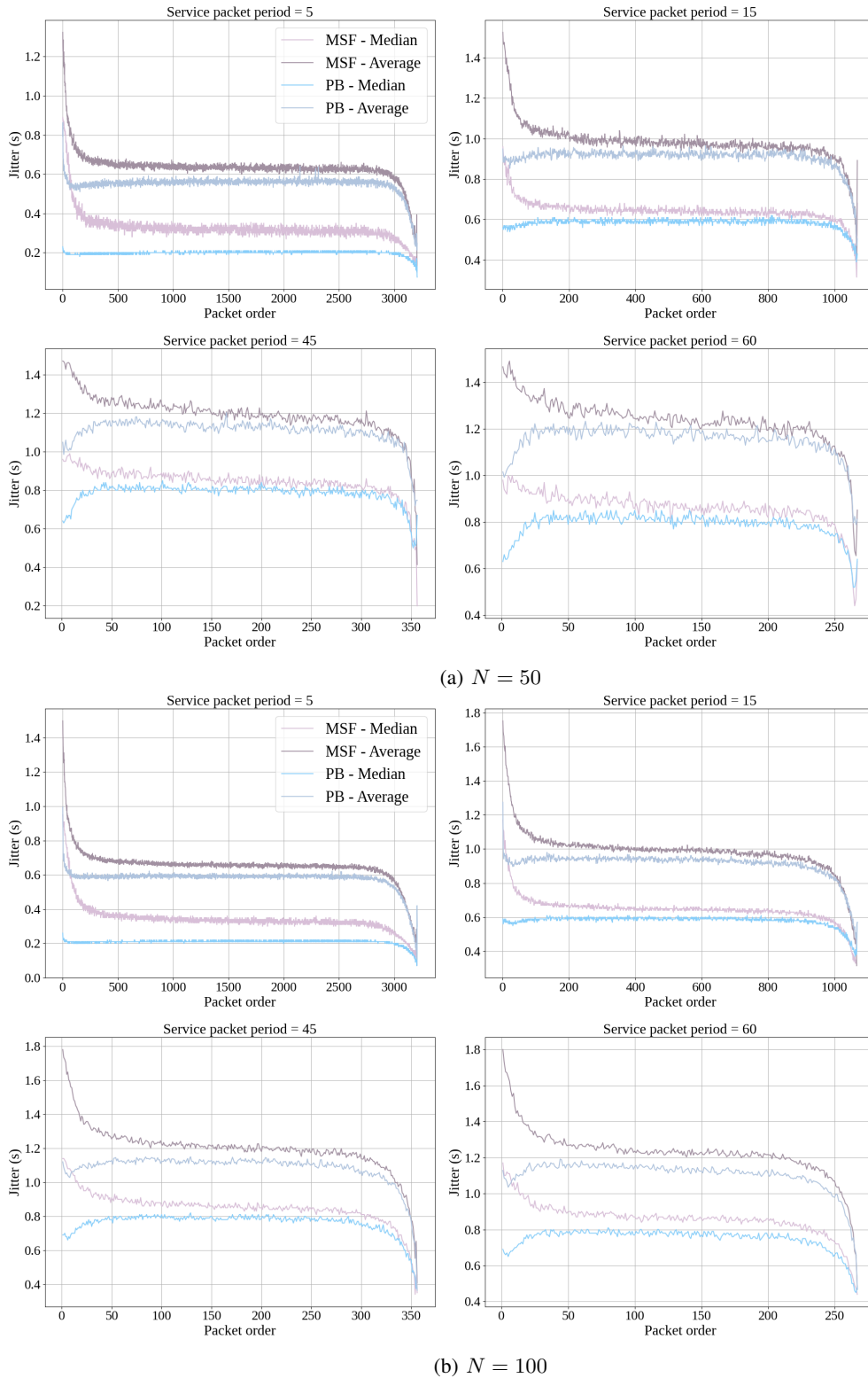
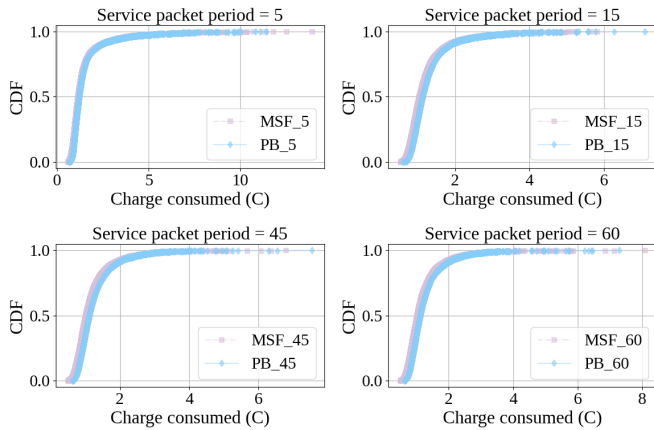


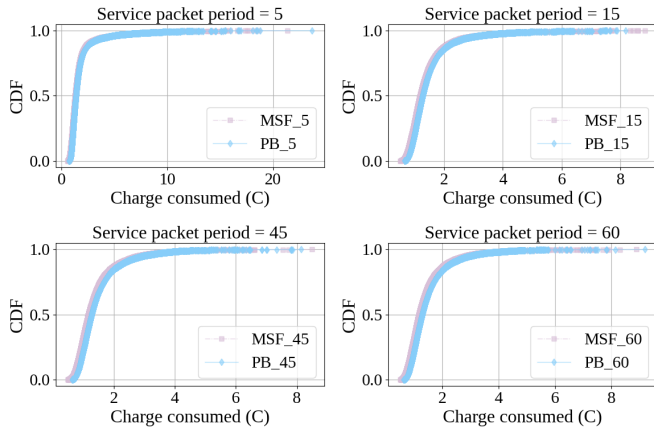
Fig. 15: Median and avg. jitter for transmitted packets during 4.5 hours (different service packet periods).

stable and does not degrade. For instance, for a service packet period of 5 seconds and PB scheme, the average jitter is at 0.6 seconds for $N = 50$ and $N = 100$. However, we notice that for $N = 50$, variations in median jitter is slightly higher than for $N = 100$. This might be due to the fixed slotframe length

that might not be suitable for any network size. For a given N , the jitter degrades with the service packet period. Indeed, a longer service time impacts packet transmissions and thus might cause additional delay and/or instability. In summary, the jitter is slightly impacted by the size of the network, while



(a) $N = 50$



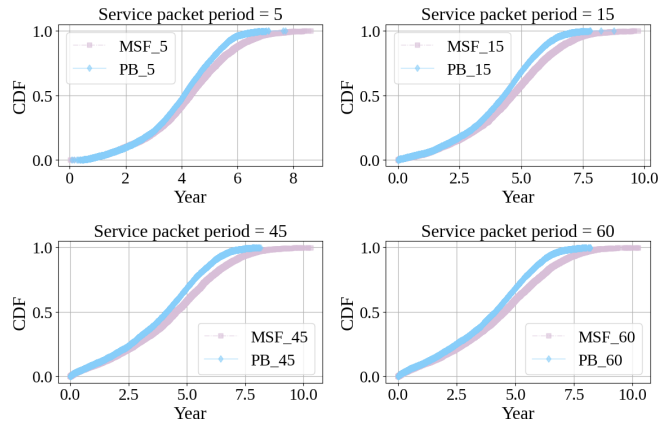
(b) $N = 100$

Fig. 16: CDF of consumed charge.

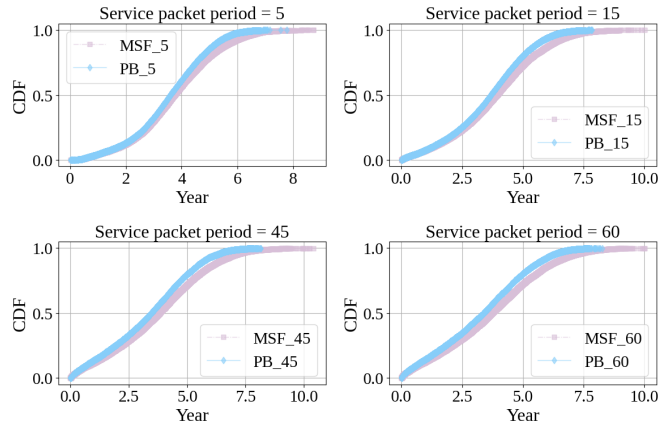
the influence of the service packet delay is more significant on both the average and median jitters.

Fig. 16 presents the Cumulative Distribution Function (CDF) as a function of the charge consumed (in Coulomb) for the PB (blue) and MSF (purple) solutions, for different N and service packet periods. For any scenario, the charge consumption profiles of PB and MSF are almost identical. This result emphasizes the efficiency of our solution in conserving energy similarly to MSF, while realizing significant improvements in terms of other performance metrics, such as joining time, E2E latency, and jitter. We note that for a given N , when the service packet period increases, the CDF's slope is almost the same. This means that the amount of charge consumed by a node in the network is not affected by the service packet period. Also, the CDF between $N = 50$ and $N = 100$ at a fixed service packet period are very similar. Hence, N has a negligible impact on the consumed charge per node.

In Fig. 17, we evaluate the CDF of the lifetime of the network's nodes for the PB (blue) and MSF (purple) solutions, for different N and service packet periods. For any N and service packet period value, the lifetime of nodes in the PB-based network is slightly lower than that of the MSF-based one. For instance, for $N = 50$ and service packet period equal to 45, we see that 67% of the nodes will have a lifetime of less than 5 years using PB, while this proportion is only 58%



(a) $N = 50$



(b) $N = 100$

Fig. 17: CDF of nodes' lifetime.

for MSF. When N increases, the gap between PB and MSF gets lower, which highlights the capability of our method to save energy in dense networks.

V. CONCLUSION

Our research introduces a novel approach to enhance 6TiSCH network performances by carefully optimizing the interaction between SF and RPL. Through a multitude of modifications within the exchanged messages in 6TiSCH and improvements in SF and RPL operations, our proposed solution is capable of enhancing several performance metrics, including joining time, transmitted/received packet number, E2E latency, and jitter, while keeping the energy usage at levels similar to the MSF benchmark and nodes' lifetime. Despite the realized improvements, several challenges remain to be solved. For instance, the fixed duration of time slots prevents the network from achieving its full potential.

ACKNOWLEDGMENT

This work was supported by funding from the Algerian Ministry of Higher Education and Scientific Research.

REFERENCES

- [1] A. Baiyere, H. Topi, V. Venkatesh, J. Wyatt, and B. Donnellan, "The internet of things (iot) - a research agenda for information systems," *Communications of the Association for Information Systems*, vol. 47, 05 2020.
- [2] D. De Guglielmo, S. Brienza, and G. Anastasi, "IEEE 802.15.4e: A survey," *Computer Communications*, vol. 88, pp. 1–24, 2016.
- [3] D. Guglielmo, G. Anastasi, and A. Seghetti, "From ieee 802.15.4 to ieee 802.15.4e: A step towards the internet of things," *Advances in Intelligent Systems and Computing*, vol. 260, pp. 135–152, 03 2014.
- [4] J. Adriano, E. C. Rosário, and J. Rodrigues, "Wireless sensor networks in industry 4.0: Wirelesshart and isa100.11a," in *Proc. IEEE Int. Conf. Indus. Appl. (INDUSCON)*, 11 2018, pp. 924–929.
- [5] N. Choudhury, R. Matam, M. Mukherjee, and J. Lloret, "A performance-to-cost analysis of ieee 802.15.4 mac with 802.15.4e mac modes," *IEEE Access*, vol. 8, pp. 41 936–41 950, 2020.
- [6] "Ieee standard for low-rate wireless networks," *IEEE Std 802.15.4-2015 (Revision of IEEE Std 802.15.4-2011)*, pp. 1–709, 2016.
- [7] T. Chang, M. Vučinić, X. Vilajosana, S. Duquennoy, and D. R. Dujovne, "6TiSCH minimal scheduling function (MSF)," RFC 9033, May 2021. [Online]. Available: <https://www.rfc-editor.org/info/rfc9033>
- [8] P. Thubert, "Objective Function Zero for the Routing Protocol for Low-Power and Lossy Networks (RPL)," RFC 6552, Mar. 2012. [Online]. Available: <https://www.rfc-editor.org/info/rfc6552>
- [9] A. Tabouche, B. Djamaa, and M. R. Senouci, "Traffic-Aware Reliable Scheduling in TSCH Networks for Industry 4.0: A Systematic Mapping Review," *IEEE Communications Surveys & Tutorials*, pp. 1–1, 2023. [Online]. Available: <https://ieeexplore.ieee.org/document/10208136/>
- [10] X. Vilajosana, K. Pister, and T. Watteyne, "Minimal IPv6 over the TSCH Mode of IEEE 802.15.4e (6TiSCH) Configuration," RFC 8180, May 2017. [Online]. Available: <https://www.rfc-editor.org/info/rfc8180>
- [11] T. Chang, M. Vučinić, X. Vilajosana, S. Duquennoy, and D. R. Dujovne, "6TiSCH Minimal Scheduling Function (MSF)," Internet Engineering Task Force, Internet-Draft draft-ietf-6tisch-msf-10, 2019, work in Progress. [Online]. Available: <https://datatracker.ietf.org/doc/html/draft-ietf-6tisch-msf-10>
- [12] P. Levis, T. H. Clausen, O. Gnawali, J. Hui, and J. Ko, "The Trickle Algorithm," RFC 6206, Mar. 2011. [Online]. Available: <https://www.rfc-editor.org/info/rfc6206>
- [13] Q. Wang, X. Vilajosana, and T. Watteyne, "6TiSCH Operation Sublayer (6top) Protocol (6P)," RFC 8480, Nov. 2018. [Online]. Available: <https://www.rfc-editor.org/info/rfc8480>
- [14] M. Rady, Q. Lampin, D. Barthel, and T. Watteyne, "6DYN: 6TiSCH with heterogeneous slot durations," *Sensors*, vol. 21, no. 5, p. 1611, Feb. 2021.
- [15] G. Daneels, D. Van Leemput, C. Delgado, E. De Poorter, S. Latré, and J. Famaey, "Parent and PHY selection in slot bonding IEEE 802.15.4e TSCH networks," *Sensors*, vol. 21, p. 5150, Jul. 2021.
- [16] D. Fanucchi, B. Staehle, and R. Knorr, "Network formation for industrial IoT: Evaluation, limits and recommendations," in *Proc. IEEE Int. Conf. Emerg. Technol. Factory Automation (ETFA)*, vol. 1, 2018, pp. 227–234.
- [17] A. Kalita and M. Khatua, "Opportunistic transmission of control packets for faster formation of 6TiSCH network," *ACM Trans. IoT*, vol. 2, no. 1, pp. 1–29, Feb. 2021.
- [18] Y. Tanaka, P. Minet, M. Vučinić, X. Vilajosana, and T. Watteyne, "Ysf: A 6tisch scheduling function minimizing latency of data gathering in iiot," *IEEE Internet of Things Journal*, vol. 9, no. 11, pp. 8607–8615, 2022.
- [19] G. Daneels, B. Spinnewyn, S. Latré, and J. Famaey, "ReSF: recurrent low-latency scheduling in IEEE 802.15.4e TSCH networks," *Ad Hoc Netw.*, vol. 69, pp. 100–114, 2018.
- [20] W. Yang, Y. Cao, H. Wang, Z. Zhang, and C. Wu, "EDSF: efficient distributed scheduling function for IETF 6TiSCH-based industrial wireless networks," *Mob. Netw. & Appl.*, Jun. 2022.
- [21] S. Jeong, J. Paek, H.-S. Kim, and S. Bahk, "TESLA: Traffic-aware elastic slotframe adjustment in TSCH networks," *IEEE Access*, vol. 7, pp. 130 468–130 483, Sept. 2019.
- [22] X. Fafoutis, A. Elsts, G. C. Oikonomou, R. J. Piechocki, and I. Craddock, "Adaptive static scheduling in IEEE 802.15.4 TSCH networks," in *Proc. IEEE World Forum IoT (WF-IoT)*, 2018, pp. 263–268.
- [23] A. R. Urke, O. Kure, and K. Ovsthus, "A survey of 802.15.4 TSCH schedulers for a standardized industrial internet of things," *Sensors*, vol. 22, no. 1, 2022.
- [24] S. Kharb and A. Singhrova, "A survey on network formation and scheduling algorithms for time slotted channel hopping in industrial networks," *J. Netw. & Computer Appl.*, vol. 126, pp. 59–87, 2019.
- [25] B. Aydın, S. Görmüş, H. Aydın, and S. Külcü, "A new routing objective function for IETF 6TiSCH protocol," in *Proc. Sig. Process. Commun. Appl. Conf. (SIU)*, 2022, pp. 1–4.
- [26] T. Bekar, S. Görmüş, B. Aydın, and H. Aydın, "Q-learning algorithm inspired objective function optimization for IETF 6TiSCH networks," in *Proc. Int. Conf. Smart Appl. Commun. Network. (SmartNets)*, 2023, pp. 1–6.
- [27] A. Kalita, A. Hazra, and M. Gurusamy, "Efficient schemes for improved performance in 6TiSCH networks," in *Proc. IEEE Conf. Computer Commun. Wrkshps. (INFOCOM WKSHPS)*, 2023, pp. 1–6.
- [28] T. Watteyne, M. R. Palattella, and L. A. Grieco, "Using IEEE 802.15.4e Time-Slotted Channel Hopping (TSCH) in the Internet of Things (IoT): Problem Statement," RFC 7554, May 2015. [Online]. Available: <https://www.rfc-editor.org/info/rfc7554>
- [29] R. Alexander, A. Brandt, J. Vasseur, J. Hui, K. Pister, P. Thubert, P. Levis, R. Struik, R. Kelsey, and T. Winter, "RPL: IPv6 Routing Protocol for Low-Power and Lossy Networks," RFC 6550, Mar. 2012. [Online]. Available: <https://www.rfc-editor.org/info/rfc6550>
- [30] X. Vilajosana, Q. Wang, F. Chraim, T. Watteyne, T. Chang, and K. Pister, "A realistic energy consumption model for tsch networks," *Sensors Journal, IEEE*, vol. 14, pp. 482–489, 02 2014.
- [31] T. Chang, T. Watteyne, Q. Wang, and X. Vilajosana, "LLSF: Low latency scheduling function for 6TiSCH networks," in *Proc. Int. Conf. Dist. Comput. Sensor Syst. (DCOSS)*, 2016, pp. 93–95.
- [32] E. Municio, G. Daneels, M. Vučinić, S. Latré, J. Famaey, Y. Tanaka, K. Brun, K. Muraoka, X. Vilajosana, and T. Watteyne, "Simulating 6TiSCH networks," *Trans. Emerg. Telecommun. Technol.*, vol. 30, no. 3, p. e3494, 2019.